Adsorption of Hydrophobic Polyelectrolytes at Oppositely Charged Surfaces

Andrey V. Dobrynin*,† and Michael Rubinstein

Department of Chemistry, University of North Carolina, Chapel Hill, North Carolina 27599-3290

Received August 20, 2001

ABSTRACT: We develop a scaling theory of adsorption of necklace-like hydrophobic polyelectrolytes at an oppositely charged hydrophilic and hydrophobic surfaces. At low surface charge densities we predict a two-dimensional adsorbed layer with thickness determined by the balance between electrostatic attraction to the charged surface and chain entropy. At high surface charge densities we expect a 3-dimensional layer with polymer density profile determined either by the balance between two-body monomer−monomer attraction or by electrostatic attraction to the surface and three-body monomer−monomer repulsion. These different stabilizing mechanisms result in the nonmonotonic dependence of the layer thickness on the surface charge density. For adsorption of polyelectrolyte chains from salt solutions the screening of the electrostatic repulsion between adsorbed polyelectrolyte chains results in large overcompensation of the surface charge for two-dimensional adsorbed layers. The polymer surface coverage for this regime increases with increasing salt concentration. The opposite trend is predicted for 3-D adsorbed layers where the polyelectrolyte surface excess decreases with increasing salt concentration.

1. Introduction

Polyelectrolytes are polymers with ionizable groups that in solutions with high dielectric constant (e.g., in aqueous solutions) dissociate, releasing counterions into solutions and leaving charged monomers on polymer backbones.[1,2] The intramolecular electrostatic repulsion between charged monomers forces chains to adopt elongated conformations. The behavior of polyelectrolytes in solutions strongly depends on the solvent quality for polymer backbone. In a good or Θ-solvent the chain size can be estimated from the balance of the chain elasticity and electrostatic repulsion between charged monomers.[3−6] Polyelectrolyte size increases with increasing fraction of charged monomers on polymer chains. The situation is qualitatively different for polyelectrolytes in a poor solvent. The shape of these polymers is determined by the interplay between electrostatic and polymer−solvent interactions. Polyelectrolyte chains in a poor solvent adopt a necklace-like structure of beads connected by narrow strings[7−14] as a compromise between electrostatic and surface energies. Larger polymeric globules break up into smaller ones with increasing fraction of charged monomers on the chain. The surface energy of the polymer−solvent interface in equilibrium globules is balanced by the electrostatic repulsion between charged monomers.

The necklace-like structure was shown to manifest itself in unique scaling laws in semidilute polyelectrolyte solutions for the concentration range where the correlation length ξ of a solution is of the order of the string length between two neighboring beads.[9] In this concentration range the correlation length ξ decreases with polymer concentration c as $\xi \sim c^{-1/3}$, viscosity is concentration-independent, and self-diffusion coefficient D increases with concentration $D \sim c^{1/3}$ in both unentangled and entangled solutions. Another interesting feature of the pearl necklace structure is the sawtooth force−extension curve predicted for hydrophobic polyelectrolytes under the applied external force.[15−17] This type of force−extension curve formally corresponds to the abrupt transitions between necklaces with different number of beads resulting in a series of abrupt length jumps with increasing applied force.

The next step toward a complete picture of polyelectrolytes in a poor solvent is to provide a theoretical framework for understanding their behavior at surfaces and interfaces. The latest progress in the theory of polyelectrolyte adsorption[18−22] provides an unique opportunity to apply these results to adsorption of necklace-like molecules. In the present paper we develop a theory of adsorption of polyelectrolytes from a poor solvent at an oppositely charged hydrophilic and hydrophobic surfaces and calculate the adsorption diagrams of these systems as functions of the surface charge density and the salt concentration.

The paper is organized as follows. In the next section we briefly review the necklace model of polyelectrolytes in a poor solvent and estimate the free energy due to confinement of a necklace molecule into a slit between parallel plates. Sections 3−5 discuss the adsorption of hydrophobic polyelectrolytes at hydrophilic surfaces when polymer adsorption is caused exclusively by electrostatic interactions between adsorbing surface and oppositely charged polyelectrolytes. In sections 3 and 4 we apply the concept of the strongly correlated Wigner liquid[21−26] to describe the structure of dilute and semidilute adsorbed layers formed by necklace-like chains. In section 5 we use a mean-field approach[21−23,27−29] to calculate polymer density profile and surface coverage for concentrated adsorbed layers of overlapping beads. In section 6 we discuss the effects of van der Waals attractions between adsorbing surface and polymer backbones on its adsorption and calculate the adsorption diagram for the case of adsorption of hydrophobic polyelectrolytes at hydrophobic oppositely charged surfaces.

† Permanent address: Institute of Materials Science and Department of Physics, University of Connecticut, Storrs, CT 06269-3136.

10.1021/ma0114943 CCC: $22.00
Published on Web 02/22/2002

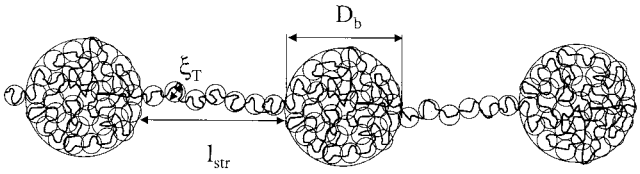

Figure 1. Polyelectrolyte chain in a dilute salt-free solution. See text for definition of length scales.

2. Necklace Model of a Polyelectrolyte Chain in a Poor Solvent[7,9]

A polyelectrolyte chain with degree of polymerization N, fraction of charged monomers f, and bond length a in a poor solvent forms a necklace-like globule of beads connected by narrow strings[7,9] (see Figure 1). The monomer density ρ inside these globules is determined by the balance between the two-body attraction $-\tau a^3\rho N$, where the reduced temperature is given by

$$\tau = (\Theta - T)/\Theta \tag{1}$$

and Θ is the theta temperature for a polymer backbone in a given solvent, and the three-body repulsion $a^6\rho^2 N$. The resulting density inside the globules is

$$\rho \approx \tau/a^3 \tag{2}$$

The shape of a globule is determine by the competition between electrostatic repulsion between charged monomers and the surface energy of the globule. The size of the beads

$$D_b \approx a(uf^2)^{-1/3} \tag{3}$$

is determined by the Rayleigh's stability condition[30]

$$l_B f^2 m_b^2/D_b \approx D_b^2 \xi_T^{-2} \tag{4}$$

where

$$m_b \approx \frac{\tau}{uf^2} \tag{5}$$

is the number of monomers in a bead ($m_b \approx \rho D_b^3$), $l_B = e^2/(kT\epsilon)$ is the Bjerrum length, and u is the ratio of the Bjerrum length l_B (the length scale at which electrostatic interaction between two elementary charges e in the media with dielectric constant ϵ is of the order of the thermal energy kT) to the bond size a. The diameter of the strings is of the order of the thermal blob size

$$\xi_T \approx a/\tau \tag{6}$$

The length l_{str} of a string connecting two neighboring beads can be estimated by balancing the electrostatic repulsion between two closest beads $kTl_B f^2 m_b^2/l_{str}$ and the surface energy of the string kTl_{str}/ξ_T. The equilibrium distance between beads is

$$l_{str} \approx a\left(\frac{\tau}{uf^2}\right)^{1/2} \approx a m_b^{1/2} \tag{7}$$

The mass of a string between neighboring beads $m_{str} \approx \rho l_{str}\xi_T^2$ is much smaller than the mass of a bead m_b

$$\frac{m_{str}}{m_b} \approx \left(\frac{uf^2}{\tau^3}\right)^{1/2} \ll 1 \tag{8}$$

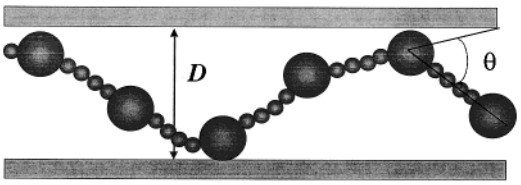

Figure 2. Necklace in a slit.

In this case the number of beads N_{bead} on the chain is approximately equal to $N/m_b \approx uf^2N/\tau$. Since most of the necklace length is due to the strings ($l_{str} > > D_b$), the length of the necklace can be estimated as the number of beads N_{bead} per chain times the length of a string l_{str} between neighboring beads

$$L_{nec} \approx N_{bead} l_{str} \approx a\left(\frac{uf^2}{\tau}\right)^{1/2} N \approx a\frac{N}{m_b^{1/2}} \tag{9}$$

Within this approximation the total free energy of the polyelectrolyte chain in a poor solvent is

$$\frac{W_{nec}}{kT} \approx N\frac{l_B f^2 m_b}{D_b} + \frac{l_B f^2 N^2}{L_{nec}} - N\tau^2 \tag{10}$$

where the first term is the electrostatic and surface energies of the beads, the second one is the electrostatic repulsion between beads which is of the order of the surface energy of the strings, and the last one is the free energy of a polymer backbone in a poor solvent. The electrostatic repulsion between beads (the second term on the right-hand side of eq 10) is smaller than the electrostatic energy of the beads (the first term) and can be neglected as long as the length of the string l_{str} between two neighboring beads is larger than the bead size D_b.

$$\frac{W_{nec}}{kT} \approx N(uf^2)^{1/3}\tau - N\tau^2 \tag{11}$$

The transverse size of the polyelectrolyte chain in a poor solvent can be estimated by considering the electrostatic energy change of any three consecutive beads due to conformational bent by an angle θ from a straight alignment (see Figure 2). The variation of the electrostatic repulsion between beads due to such deformation is

$$\frac{\delta W_{el}}{kT} \approx \frac{l_B(fm_b)^2}{l_{str}}\left(\frac{1}{\sqrt{4\cos^2\theta + \sin^2\theta}} - \frac{1}{2}\right) \approx \frac{l_B(fm_b)^2}{l_{str}}\theta^2 \approx \frac{l_{str}}{\xi_T}\theta^2 \tag{12}$$

Thus, the mean-square value of the bending angle is $\langle\theta^2\rangle \approx \xi_T/l_{str}$. The mean-square transverse size $\langle R_\perp^2\rangle$ of the polyelectrolyte chain with a sequence of bending angles θ_i is

$$\langle R_\perp^2\rangle \approx l_{str}^2 \sum_{i=1}^{N_{bead}-2} \langle\theta_i^2\rangle \approx \frac{N}{m_b} l_{str}\xi_T \approx a^2 N\left(\frac{uf^2}{\tau^3}\right)^{1/2} \tag{13}$$

The transverse size of a polyelectrolyte chain in a poor solvent is smaller than that in a Θ-solvent $a\sqrt{N}$ because $\tau^3 > uf^2$.

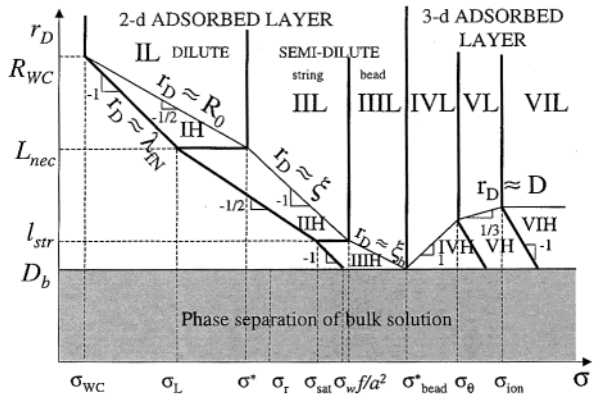

Figure 3. Adsorption diagram of polyelectrolyte chains in a salt solution as a function of surface charge density σ and Debye radius r_D. The thin solid line separates low and high salt regimes.

The confinement energy of a polyelectrolyte chain in a poor solvent with transverse size $\sqrt{\langle R_\perp^2 \rangle}$ in a slit of size D (see Figure 2) can be estimated as

$$\frac{F_{conf}}{kT} \approx \frac{\langle R_\perp^2 \rangle}{D^2} \approx \left(\frac{uf^2}{\tau^3}\right)^{1/2} \frac{a^2 N}{D^2} \tag{14}$$

3. Dilute Two-Dimensional Wigner Liquid

Consider adsorption of polyelectrolyte chains at an oppositely charged surface with number density of surface charge σ from a dilute polymer solution with polymer concentration ρ_{bulk} and with salt concentration ρ_{salt}. The presence of the univalent salt at concentration ρ_{salt} leads to an exponential screening of the electrostatic interactions at the length scales of the order of the Debye screening length

$$r_D = (8\pi l_B \rho_{salt})^{-1/2} \tag{15}$$

In Figure 3 we sketch the adsorption diagram of polyelectrolyte chains at an oppositely charged surface with number density of surface charges σ−Debye length r_D plane.

The structure of the adsorbed polyelectrolyte layer at low surface charge densities can be described using the concept of the strongly correlated Wigner liquid.[24−26] In the framework of this approach the polyelectrolyte chains are considered to be localized at the centers of the Wigner−Seitz cells of size R. The total electrostatic energy of an adsorbed polyelectrolyte chain includes the electrostatic attraction of the chain to the oppositely charged surface

$$\frac{W_{att}}{kT} \approx -l_B f N \sigma \int_0^\infty dr \exp\left(-\frac{r}{r_D}\right) \approx -l_B f N \sigma r_D \tag{16}$$

and repulsion from other adsorbed polyelectrolytes distributed with effective surface charge density fN/R^2 starting at distance R from a given polyion

$$\frac{W_{rep}}{kT} \approx \frac{l_B (fN)^2}{R^2} \int_R^\infty dr \exp\left(-\frac{r}{r_D}\right) \approx \frac{l_B (fN)^2 r_D}{R^2} \exp\left(-\frac{R}{r_D}\right) \tag{17}$$

The total electrostatic energy of the adsorbed layer with the surface area S is the sum of the contributions from all chains

$$\frac{U}{kT} \approx \frac{S}{R^2}\left(\frac{1}{2}\frac{W_{rep}}{kT} + \frac{W_{att}}{kT}\right) \approx S l_B r_D f N \left(\frac{1}{2}\frac{fN}{R^4}\exp\left(-\frac{R}{r_D}\right) - \frac{\sigma}{R^2}\right) \tag{18}$$

(The factor $^1/_2$ in front of the repulsive term W_{rep} is added to avoid the double counting of the electrostatic repulsion between adsorbed chains.) The dependence of the Wigner−Seitz cell size R on the salt concentration is derived by minimizing the electrostatic energy U with respect to the cell size R. This minimization leads to the following equation for the cell size R

$$\frac{fN}{R^2}\exp\left(-\frac{R}{r_D}\right)\left(1 + \frac{1}{4}\frac{R}{r_D}\right) \approx \sigma \tag{19}$$

Low Salt Regime (Regime IL in Figure 3). At low salt concentrations ($r_D > R$) we can expand the terms on the left-hand side of eq 19 in the power series of the ratio of the Wigner−Seitz cell size R to the Debye radius r_D. Within the zeroth approximation the size of the Wigner−Seitz cell

$$R \approx R_0 \approx \sqrt{fN/\sigma}, \quad \text{low salt } r_D > \sqrt{fN/\sigma} \tag{20}$$

is independent of the Debye screening length. To obtain the surface overcharging $\delta\sigma$, one has to keep the first-order term in the powers of R/r_D on the left-hand side of eq 19. Within this approximation the overcharging of the surface by adsorbed polyelectrolyte chains is[19,22]

$$\delta\sigma \approx \frac{fN}{R^2} - \sigma \approx \sigma \frac{R_0}{r_D}, \quad \text{low salt } r_D > \sqrt{fN/\sigma} \tag{21}$$

It follows from this equation that the effective surface charge density $\delta\sigma$ at the crossover between dilute low (IL) and dilute high (IH) salt regimes (at $r_D \approx R \approx \sqrt{fN/\sigma}$ (see the crossover line in Figure 3) is of the order of the bare surface charge density σ, but has an opposite sign.

From the equilibrium cell size R_0 one can estimate the adsorption energy of the polyelectrolyte chain with the center of mass located at the distance z ($z \ll R_0$) from the surface as the energy of the electrostatic attraction between a charged disk of radius R_0 and a charge of valency fN

$$W_{ads}(z) \approx -kT l_B (fN)^{3/2} \sigma^{1/2}\left(1 - \frac{z}{R_0}\right), \quad \text{low salt } r_D > \sqrt{fN/\sigma} \tag{22}$$

The polyelectrolyte chains are strongly attracted to the surface with the binding energy

$$|W_{ads}(0)| \approx kT l_B (fN)^{3/2} \sigma^{1/2} \approx (\sigma/\sigma_{WC})^{1/2} \gg kT \tag{23}$$

as long as the surface charge density σ is larger than the adsorption threshold value σ_{WC}

$$\sigma_{WC} \approx \frac{1}{l_B^2 (fN)^3} \tag{24}$$

The chains are localized within a layer of thickness

$$D \approx \frac{R_0}{l_B(fN)^{3/2}\sigma^{1/2}} \approx (l_B fN\sigma)^{-1}, \quad \text{low salt } r_D > \sqrt{fN/\sigma} \tag{25}$$

inside which (for $z < D$) the change of the adsorption energy $W_{ads}(0) - W_{ads}(z)$ (eq 22) is of the order of the thermal energy kT.

The strong electrostatic attraction of polyelectrolyte chains to the charged surface starts to deform them when the layer thickness D (eq 25) becomes comparable with the transverse size of the chains $\sqrt{\langle R_\perp^2 \rangle}$ (see eq 13). This occurs at the surface charge density

$$\sigma_{def} \approx \frac{\tau^{3/4}}{a^2 u^{5/4} f^{3/2} N^{3/2}} \tag{26}$$

At higher surface charge densities $\sigma > \sigma_{def}$ the thickness of the chains in the direction perpendicular to the surface is determined by balancing the confinement entropy of a polyelectrolyte chain in a poor solvent (eq 14) inside the layer of the thickness D with its electrostatic attraction $W_{ads}(D)$ (see eq 22) to the charged surface. This gives the equilibrium thickness of the chain

$$D \approx a^{1/3} u^{-1/6} \tau^{-1/2} \sigma^{-1/3} \tag{27}$$

that is independent of the degree of polymerization N.

High Salt Regime (Regime IH in Figure 3). If the Debye radius r_D becomes smaller than $\sqrt{fN/\sigma}$, the adsorbed polyelectrolyte chains interact only with the part of the surface within the Debye screening length r_D. The Wigner−Seitz cell size R that minimizes the electrostatic energy eq 18 is

$$R \approx r_D \ln\left(\frac{fN}{\sigma r_D^2}\right), \quad \text{high salt } r_D < \sqrt{fN/\sigma} \tag{28}$$

Thus, up to logarithmic prefactor the cell size R is proportional to the Debye radius r_D.[19,21] The effective surface charge density in this high salt concentration regime is

$$\delta\sigma \approx \frac{fN}{R^2} \approx \frac{fN}{\left(r_D \ln\left(\frac{fN}{\sigma r_D^2}\right)\right)^2} \approx \frac{fN}{r_D^2}, \quad \text{high salt } r_D < \sqrt{fN/\sigma} \tag{29}$$

and can be much larger than the bare surface charge density σ.

As the salt concentration increases, the Debye radius decreases and the absolute value of the attractive energy of the polyelectrolyte chain to the charged surface $l_B fN\sigma r_D$ decreases as well. Polyelectrolyte chains desorb from the charged surface when this energy becomes of the order of the thermal energy kT. At this value of the adsorption energy the concentration of polyelectrolyte chains at the surface is of the order of polymer concentration in the bulk. In dilute high salt (regime IH) desorption occurs if the Debye radius r_D is of the order of the thickness of the adsorbed layer eq 25. The line

$$r_D^{des} \approx \lambda_{fN} \approx (l_B fN\sigma)^{-1}, \quad \text{high salt } r_D < \sqrt{fN/\sigma} \tag{30}$$

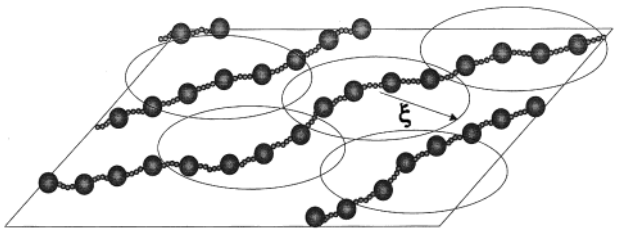

Figure 4. Schematic sketch of the adsorbed layer in *semidilute string-controlled 2-D* regime.

defines the desorption threshold for nonoverlapping (dilute) adsorbed polyelectrolyte chains (left boundary of regime IH in Figure 3).

4. Semidilute Two-Dimensional Wigner Liquid

4.1. String-Controlled Regime (Regime II). The adsorbed polyelectrolytes begin to overlap when the size of the Wigner−Seitz cell R is of the order of the chain size L_{nec} (eq 9). At low salt concentrations ($r_D > \sqrt{fN/\sigma}$) the chains begin to overlap at the surface charge density

$$\sigma^* \approx \frac{\tau}{ua^2 fN}, \quad \text{low salt } r_D > \sqrt{fN/\sigma} \tag{31}$$

For higher surface charge densities ($\sigma > \sigma^*$) the adsorbed polyelectrolytes are arranged in a two-dimensional semidilute polyelectrolyte solution with the distance between chains ξ (see Figure 4). Polyelectrolyte chains are strongly stretched by intrachain electrostatic repulsion on length scales smaller than the cell size ξ. The number of monomers inside the cell g_ξ is

$$g_\xi \approx \frac{N\xi}{L_{nec}} \approx \xi \tau^{1/2} a^{-1} u^{-1/2} f^{-1} \tag{32}$$

To calculate the electrostatic energy of the adsorbed layer, we will once again divide the electrostatic contribution to the total electrostatic energy of the adsorbed chains into the repulsive and the attractive ones. The electrostatic energy of the adsorbed layer can be written by analogy with eq 18 by substituting g_ξ for N and ξ for R, which leads to

$$\frac{U}{kT} \approx Sl_B r_D f g_\xi \left(\frac{fg_\xi}{2\xi^4} \exp\left(-\frac{\xi}{r_D}\right) - \frac{\sigma}{\xi^2}\right) \tag{33}$$

Minimizing the total electrostatic energy U of the adsorbed layer with respect to the Wigner−Seitz cell size ξ, we obtain an equation that defines the cell size as a function of the Debye radius r_D and the surface charge density σ

$$\frac{\tau^{1/2}}{u^{1/2}\xi a}\left(1 + \frac{\xi}{2r_D}\right) \exp\left(-\frac{\xi}{r_D}\right) \approx \sigma \tag{34}$$

At low salt concentrations (regime IIL) the size of the cell

$$\xi \approx \frac{\tau^{1/2}}{u^{1/2} a\sigma}, \quad \text{low salt } r_D > \tau^{1/2}/(u^{1/2} a\sigma) \tag{35}$$

is inversely proportional to the surface charge density σ, and the surface overcharging $\delta\sigma$ in this regime is

$$\delta\sigma \approx \sigma\left(\frac{\xi}{r_D}\right) \approx \frac{\tau^{1/2}}{u^{1/2} r_D a}, \quad \text{low salt } r_D > \tau^{1/2}/(u^{1/2}a\sigma) \quad (36)$$

Surface overcharging $\delta\sigma$ is inversely proportional to the Debye radius r_D and is independent of the surface charge density σ.

For high salt concentrations (regime IIH) the solution of eq 34 is

$$\xi \approx r_D \ln\left(\frac{\tau^{1/2}}{\sigma r_D a u^{1/2}}\right), \quad \text{high salt } r_D < \tau^{1/2}/(u^{1/2}a\sigma) \quad (37)$$

The surface overcharging by the adsorbed polyelectrolyte chains at high salt concentrations

$$\delta\sigma \approx \frac{f g_\xi}{\xi^2} - \sigma \approx \frac{\tau^{1/2}}{u^{1/2} a r_D \ln\left(\frac{\tau^{1/2}}{\sigma r_D a u^{1/2}}\right)} \approx \frac{\tau^{1/2}}{u^{1/2} r_D a}, \quad \text{high salt } r_D < \tau^{1/2}/(u^{1/2}a\sigma) \quad (38)$$

has the same functional form with logarithmic accuracy as eq 36 for low salt concentrations. However, it is important to point out that at low salt concentrations the surface overcharging $|\delta\sigma|$ is much smaller than the bare surface charge density σ, while at higher salt concentrations $|\delta\sigma| > \sigma$.

The thickness of the adsorbed layer D in regime II is still given by eq 27 and decreases with increasing surface charge density as $\sigma^{-1/3}$. This decrease continues while the thickness of the polyelectrolyte layer is larger than the bead size D_b (eq 3) or as long as the surface charge density σ is smaller than

$$\sigma_{sat} \approx \frac{u^{1/2} f^2}{a^2 \tau^{3/2}} \quad (39)$$

For higher surface charge densities $\sigma > \sigma_{sat}$ the thickness of the adsorbed layer D saturates at D_b, and the beads keep their spherical shape because the electrostatic attraction to the charged surface is weaker than the electrostatic self-energy of the beads.

Flexible hydrophobic polyelectrolyte chains with the persistence length proportional to the Debye screening length[9] r_D desorb when the electrostatic attraction between the charged surface and a section of size r_D is of the order of thermal energy[31] kT

$$|W_{ads}| \approx kT l_B \sigma f g_\xi r_D \approx kT \quad (40)$$

The desorption transition occurs at the Debye screening length[32] (lower left boundary of the regime IIH in Figure 3)

$$r_D^{des} \approx \frac{1}{u^{1/4}\tau^{1/4}\sigma^{1/2}}, \quad \text{for } r_D > l_{str} \quad (41)$$

The crossover to a rigid chain behavior takes place when the Debye screening length r_D is of the order of the chain size L_{nec}. For larger values of the Debye radius the chain can be viewed as a charged rod of length L_{nec}. The desorption of such rod occurs along the line in the adsorption diagram (left boundary of the regime IH in Figure 3) given by eq 30.

This *string-controlled* regime (regime II) continues until the Wigner−Seitz cell size ξ is larger than the distance between neighboring beads l_{str} (eq 7). The cell size ξ is comparable with the string length l_{str} at low salt concentrations for the surface charge density (boundary between regimes IIL and IIIL in Figure 3)

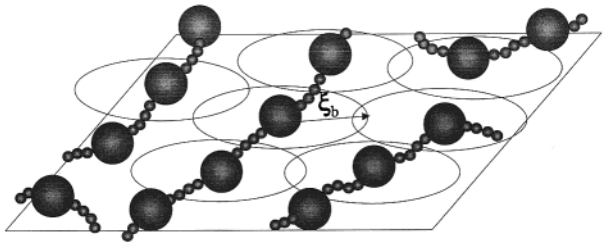

Figure 5. Schematic sketch of the adsorbed layer in *semidilute bead-controlled 2-D* regime.

$$\sigma_{bead} \approx \frac{f}{a^2}, \quad \text{low salt } r_D > \tau^{1/2}/(u^{1/2}a\sigma) \quad (42)$$

and at higher salt concentrations for the value of the Debye radius (boundary between regimes IIH and IIIH in Figure 3)

$$r_D^{bead} \approx l_{str} \approx a\left(\frac{\tau}{uf^2}\right)^{1/2}, \quad \text{high salt } r_D < \tau^{1/2}/(u^{1/2}a\sigma) \quad (43)$$

4.2. Bead-Controlled Regime (Regime III). For smaller cell sizes ($\xi < l_{str}$) there will be one bead per each correlation cell, and the adsorbed layer can be effectively viewed as 2-D dilute Wigner liquid of charged beads (see Figure 5). The electrostatic energy per bead in the dilute Wigner liquid of beads is the sum of the electrostatic attraction of the bead with the center of mass located at distance D_b from the surface to the charged background

$$W_{att} = -kTl_B r_D \sigma f m_b \quad (44)$$

and its electrostatic repulsion from other beads

$$W_{rep} = kTl_B (f m_b)^2 r_D \xi_b^{-2} \exp(-\xi_b/r_D) \quad (45)$$

Minimization of the total electrostatic energy $S(W_{att} + W_{rep}/2)/\xi_b^2$ of the adsorbed layer with respect to the cell size ξ_b results in the following equation

$$\frac{f m_b}{\xi_b^2} \exp\left(-\frac{\xi_b}{r_D}\right)\left(1 + \frac{1}{4}\frac{\xi_b}{r_D}\right) \approx \sigma \quad (46)$$

At low salt concentrations (regime IIIL) the solution of this equation for the equilibrium cell size ξ_b is

$$\xi_b \approx \sqrt{\frac{f m_b}{\sigma}} \approx \sqrt{\frac{\tau}{uf\sigma}}, \quad \text{low salt } r_D > \sqrt{\tau/(uf\sigma)} \quad (47)$$

For this range of salt concentrations the overcharging of the surface by polyelectrolyte chains is

$$\delta\sigma \approx \sigma \frac{\xi_b}{r_D}, \quad \text{low salt } r_D > \sqrt{\tau/(uf\sigma)} \quad (48)$$

At high salt concentrations (regime IIIH) the solution of eq 46 can be approximated by

$$\xi_b \approx r_D \ln\left(\frac{\tau}{uf{r_D}^2\sigma}\right), \quad \text{high salt } r_D < \sqrt{\tau/(uf\sigma)} \quad (49)$$

Thus, up to logarithmic prefactor, the cell size ξ_b is proportional to the Debye radius r_D.[19,21]

The beads begin to overlap when the Wigner−Seitz cell size ξ_b is of the order of the beads size D_b. This takes place at low salt concentrations for surface charge density σ equal to (boundary between IIIL and IVL)

$$\sigma^*_{bead} \approx \frac{\tau}{a^2}\left(\frac{f}{u}\right)^{1/3}, \quad \text{low salt } r_D > \sqrt{\tau/(uf\sigma)} \quad (50)$$

and at high salt concentrations for the value of the Debye radius r_D

$$r^*_{bead} \approx D_b \approx a(uf^2)^{-1/3}, \quad \text{high salt } r_D < \sqrt{\tau/(uf\sigma)} \quad (51)$$

Polyelectrolyte chains desorb when the electrostatic attraction of a bead to the charged surface

$$|W_{ads}| \approx kTl_B r_D \sigma f m_b \quad (52)$$

is of the order of the thermal energy kT. The adsorption/desorption threshold takes place at the Debye radius (left boundary of regime IIIH in Figure 3)

$$r_D^{des} \approx \frac{f}{\sigma a\tau}, \quad \text{for } \sigma_{sat} < \sigma < \sigma^*_{bead} \quad (53)$$

This adsorption/desorption line crosses the line $r_D \approx D_b$ at the surface charge density

$$\sigma_w \approx \frac{u^{1/3}f^{5/3}}{a^2\tau} \quad (54)$$

At this surface charge density the attraction of a bead to the surface with area D_b^2 and charge $\sigma_w D_b^2$ is of the order of kT.

At high salt concentrations with Debye radius r_D smaller than the bead size D_b the electrostatic interactions between monomers are negligible in comparison with nonelectrostatic ones (see for details ref 35). Each polyelectrolyte chain forms a spherical globule with size $R_{glob} \approx aN^{1/3}\tau^{-1/3}$. The solution of globules with concentration c higher than c_{dil}

$$c_{dil} \approx \tau a^{-3} \exp(-\tau^{4/3}N^{2/3}) \quad (55)$$

is thermodynamically unstable with respect to phase separation into polymer concentrated and dilute phases.[36] In the present paper we consider only the case of salt concentrations for which r_D is larger than the bead size D_b.

5. Three-Dimensional Adsorbed Layer

At higher surface charge densities ($\sigma > \sigma^*_{bead}$) the polyelectrolyte chains form a concentrated polymer layer near the charged surface. In this regime the distribution of the polymer density can be described within the framework of the mean-field approximation assuming that the electrostatic interactions of a polymer with effective external potential $\varphi(z)$ created by other chains and the surface dominates over the electrostatic self-energy of the chain. In this approximation the polymer density $\rho(z)$ and the small ion density $\rho_\alpha(z)$ depend only on the distance z from the charged surface. The density profile of the salt ions in the electrostatic potential $\varphi(z)$ satisfies the Boltzmann distribution

$$\rho_\pm(z) = \rho_{salt} \exp(\mp\varphi(z)) \quad (56)$$

The relation between the electrostatic potential $\varphi(z)$ and local polymer density $\rho(z)$ can be derived by assuming that the adsorbed layer is built of blobs of size $\xi(z)$. The number of monomers $g(z)$ in a blob is determined from the fact that these blobs are space-filling in the adsorbed layer $g(z) \approx \rho(z)\xi^3(z)$ and the statistics of the chain inside a blob is Gaussian $\xi^2(z) \approx a^2 g(z)$. These blobs are multivalent sections of polyions with the valency $fg(z)$. Each blob interacts with the external electrostatic potential $\varphi(z)$ with the energy of the order of thermal energy kT.

$$fg(z)\,\varphi(z) \approx 1 \quad (57)$$

This leads to the following relation between the monomer concentration $\rho(z)$ and the electrostatic potential $\varphi(z)$ at the distance z from the surface

$$\rho(z) \approx g(z)/\xi^3(z) \approx a^{-3}g(z)^{1/2} \approx a^{-3}(f\varphi(z))^{1/2} \quad (58)$$

However, polyelectrolytes are already compressed by monomer−monomer attractive interactions in a poor solvent. The external electrostatic potential $\varphi(z)$ will further compress the polyelectrolyte chains only when the interaction with external potential $f\varphi(z)$ is stronger than monomer−monomer attraction τ^2.

The electrostatic potential $\varphi(z)$ satisfies the linearized Poisson−Boltzmann equation

$$\frac{d^2\varphi(z)}{dz^2} = 4\pi l_B(\rho_-(z) - \rho_+(z) + f\rho(z)) \approx \frac{\varphi(z)}{{r_D}^2} + \frac{4\pi l_B f}{a^3}\begin{cases}\tau, \text{ for } f\varphi(z) < \tau^2 \\ \sqrt{f\varphi(z)}, \text{ for } f\varphi(z) > \tau^2\end{cases} \quad (59)$$

together with the boundary condition at the charged surface

$$\left.\frac{d\varphi(z)}{dz}\right|_{z=0} = -4\pi l_B\sigma \quad (60)$$

In eq 59 we have identified two different cases depending on the surface charge density σ: (i) layer with uniform polymer density for $f\varphi(z) < \tau^2$; (ii) nonuniform layer density for $f\varphi(z) > \tau^2$.

5.1. Layer with Uniform Density (Regime IV). In the case when $f\varphi(0) \ll \tau^2$ the polymer density $\rho(z)$ in the adsorbed layer is almost constant and is equal to that inside beads τ/a^3. The layer is built by the thermal blobs of almost constant size $\xi_T \approx a\tau^{-1}$ because electrostatic attraction of charged monomers to a charged surface is weaker than two-body attraction between sections of chains in a poor solvent. The solution of the linearized Poisson−Boltzmann equation (59) in this regime is

$$\varphi(z) \approx \frac{uf\tau{r_D}^2}{a^2}\sinh^2\left(\frac{D-z}{2r_D}\right) \quad (61)$$

The thickness D of the polymeric layer can be found from the boundary condition for the electrostatic potential

$$\frac{f\tau r_D}{a^3}\sinh\left(\frac{D}{2r_D}\right)\cosh\left(\frac{D}{2r_D}\right)\approx\sigma \quad (62)$$

In the limit of low salt concentrations $D/r_D \ll 1$ (regime IVL) this equation has a simple solution

$$D\approx r_D\,\mathrm{arcsinh}\left(\frac{a^3\sigma}{f\tau r_D}\right)\approx\frac{a^3\sigma}{f\tau},\quad \text{low salt } r_D > \frac{a^3\sigma}{f\tau} \quad (63)$$

Thus, the layer thickness in this regime scales linearly with the surface charge density σ. This can be understood by realizing that at low salt concentrations the charge of the adsorbed layer compensates the charge of the surface. The monomer concentration in the adsorbed layer is constant, and therefore the effective surface charge density of the adsorbed layer is proportional to its thickness D.

The surface undercharging by adsorbed polyelectrolytes is obtained by multiplying the polymeric charge density $f\tau a^{-3}$ in the adsorbed layer by the layer thickness D

$$\delta\sigma_D\approx\frac{f\tau D}{a^3}-\sigma\approx\frac{f\tau r_D}{a^3}\,\mathrm{arcsinh}\left(\frac{a^3\sigma}{f\tau r_D}\right)-\sigma\approx-\frac{a^6\sigma^3}{f^2\tau^2 r_D} \quad (64)$$

The addition of salt decreases the polymer adsorbed amount, because salt ions also take part in screening of the surface charge.

At high salt concentrations (regime IVH) the thickness of the adsorbed layer (solution of eq 62)

$$D\approx r_D\ln\left(\frac{a^3\sigma}{f\tau r_D}\right)\approx r_D,\quad \text{high salt } r_D < \frac{a^3\sigma}{f\tau} \quad (65)$$

is proportional to the Debye radius r_D (up to logarithmic corrections).

However, the mean-field description of the polyelectrolyte adsorbed layer presented above is incorrect at distances z from the surface larger than $D-\xi_T$ within the thermal blob ξ_T of the outer edge of the adsorbed layer. At these distances the fluctuations of the polymer density become larger than the average polymer density. This layer can be considered as a two-dimensional melt of thermal blobs of size ξ_T. The additional decrease in polymer surface coverage due to this strongly fluctuating outer layer of thermal blobs can be estimated by comparing the attraction of the blobs to the charged surface with electrostatic repulsion between them. The effective surface charge density that the last layer of thickness ξ_T feels is of the order of fa^{-2}. The attraction energy of a blob to the charged background with this surface charge density is

$$W_{att}\approx-\frac{kTl_B f\xi_T f g_T}{a^2} \quad (66)$$

The repulsion of the blob from all other blobs in this layer with the effective surface charge density $\delta\sigma_{\xi_T}$ is

$$W_{rep}\approx kTl_B(\delta\sigma_{\xi_T}+f/a^2)\,fg_T r_D \quad (67)$$

At equilibrium the total electrostatic energy per blob in the adsorbed layer $W_{att}+W_{rep}$ is of the order of the thermal energy $-kT$. The surface undercharging due to this last layer of thermal blobs is

$$\delta\sigma_{\xi_T}\approx-\frac{1}{l_B f g_T r_D}\approx-\frac{\tau^2}{l_B f r_D} \quad (68)$$

The total undercharging of the adsorbing surface by polyelectrolyte chains is

$$\delta\sigma\approx\delta\sigma_{\xi_T}+\delta\sigma_D\approx-\frac{\tau^2}{l_B f r_D}-\frac{a^6\sigma^3}{f^2\tau^2 r_D^2} \quad (69)$$

Thus, chains adsorbed in the 3-D layer undercompensate the surface charge, and polymer surface coverage always decreases with increasing the salt concentration. Polyelectrolyte chains in a poor solvent demonstrate qualitatively different behavior from 3-D adsorbed polyelectrolyte layers in Θ and good solvents for the polymer backbone.[22,23] Polyelectrolytes in Θ and good solvents show nonmonotonic dependences of the surface overcharging on salt concentrations. At low ionic strengths the surface overcharging increases with increasing salt concentration while at higher ionic strengths it decreases with salt concentration.

As we show in Appendix the uniform adsorbed layer is stable well below σ^*_{bead}. However, it has higher free energy per unit area than the free energy of the Wigner liquid of beads. Thus, at the surface charge density $\sigma\approx\sigma^*_{bead}$ there is a first-order phase transition between the Wigner liquid of beads and uniform adsorbed layer.

5.2. Nonuniform Layer Density (Regime V). The electrostatic attraction of charged monomers to the charged surface $f\varphi(0)$ becomes of the order of two-body monomer−monomer attraction τ^2 at the surface charge densities σ of the order of

$$\sigma_\theta\approx\frac{\tau^{3/2}}{a^2u^{1/2}},\quad \text{low salt } r_D > \frac{a^3\sigma}{f\tau} \quad (70)$$

and at the value of the Debye radius obtained from eqs 61 and 65 (including logarithm)

$$r_D{}^\theta\approx\frac{\tau^2}{uf\sigma a},\quad \text{high salt } r_D < \frac{a^3\sigma}{f\tau} \quad (71)$$

For higher surface charge densities ($\sigma > \sigma_\theta$) or smaller values of the Debye radius ($r_D < r_D{}^\theta$) the electrostatic potential at the charged surface $\varphi(0)$ is larger than $f^{-1}\tau^2$. There are two different regions in the adsorbed layer (see Figure 6a). The structure of the adsorbed layer close to the charged surface is similar to the one for adsorption from a Θ-solvent where polymer density profile is determined by the balance between electrostatic attraction of charged monomers to the charged surface and three-body monomer−monomer repulsion,[21,23] while the polymer density in the outer layer stays almost constant τ/a^3 and is determined by the balance between two-body attraction (poor solvent) and three-body repulsion. The solution of the Poisson−Boltzmann equation in this case is

$$\varphi(z)\approx\begin{cases}\dfrac{u^2f^3r_D^4}{a^4}\sinh^4\left(\dfrac{D-z}{4r_D}\right), & \text{for } z < h\\[2ex] \dfrac{uf\tau r_D^2}{a^2}\sinh^2\left(\dfrac{D-z}{2r_D}\right), & \text{for } z > h\end{cases} \quad (72)$$

where h is the thickness of the inner layer. The thick-

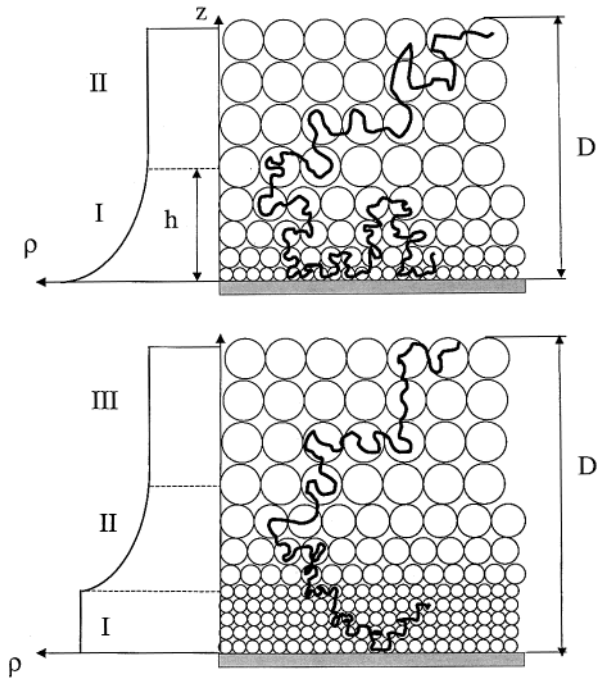

Figure 6. Polymer density profile and layer structure in the 3-D adsorbed layer: (a, top) regime V; (b, bottom) regime VI.

ness of the adsorbed layer $D = D_{out} + h$, where D_{out} is the thickness of the outer layer, can be obtained from the boundary condition eq 60

$$\frac{uf^3 r_D^3}{a^3} \sinh^3\left(\frac{D}{4r_D}\right) \cosh\left(\frac{D}{4r_D}\right) \approx \sigma a^2 \qquad (73)$$

For low salt concentrations (regime VL) the thickness of the adsorbed layer

$$D \approx a^{5/3} u^{-1/3} f^{-1} \sigma^{1/3}, \quad \text{for } \sigma_\theta < \sigma < \sigma_{ion}, \text{ low salt } r_D > D \qquad (74)$$

increases with the surface charge density as $\sigma^{1/3}$. At high salt concentrations (regime VH) the layer thickness D is of the order of the Debye radius r_D

$$D \approx r_D \ln\left(\frac{\sigma a^5}{uf^3 r_D^3}\right) \quad \text{for } \sigma_\theta < \sigma < \sigma_{ion}, \text{ high salt } r_D \approx D \qquad (75)$$

At the crossover between the inner and outer layers ($z \approx h$) the value of the electrostatic potential $\varphi(h)$ is of the order of $\tau^2 f^{-1}$. Taking this into account, we can write the expression for the thickness of the outer layer D_{out} as follows (see eq 61)

$$\sinh^2\left(\frac{D_{out}}{2r_D}\right) \approx \frac{\tau a^2}{uf^2 r_D^2} \qquad (76)$$

The solutions of this equation for low ($D_{out} < r_D$, regime VL) and high ($D_{out} \approx r_D$, regime VH) salt concentrations are

$$D_{out} \approx \begin{cases} a\sqrt{\dfrac{\tau}{uf^2}}, & \text{low salt } r_D > a\sqrt{\dfrac{\tau}{uf^2}} \\ r_D \ln\left(\dfrac{\tau a^2}{uf^2 r_D^2}\right), & \text{high salt } r_D < a\sqrt{\dfrac{\tau}{uf^2}} \end{cases} \qquad (77)$$

The inner region of the adsorbed layer of thickness h is built of the blobs with gradually increasing sizes

$$\xi(z) \approx \frac{1}{\rho(z)a^2} \approx \frac{a}{\sqrt{f\varphi(z)}} \approx \frac{a^3}{uf^2 r_D^2} \sinh^{-2}\left(\frac{D-z}{4r_D}\right) \qquad (78)$$

As the surface charge density increases, the size of the first blob $\xi(0)$ decreases. At the surface charge density

$$\sigma_{ion} \approx \begin{cases} \dfrac{f^{3/4}}{a^2 u^{1/2}}, & \text{low salt } r_D > au^{-1/2} f^{-3/4} \\ \dfrac{1}{ur_D a}, & \text{high salt } r_D < au^{-1/2} f^{-3/4} \end{cases} \qquad (79)$$

the size of this blob $\xi(0)$ is of the order of the distance between charged monomers $a/\sqrt{f}$ and there is one charged monomer per such blob. This is the maximum possible screening of the surface by polyelectrolytes. Further increase of polymer density near the surface is unfavorable due to the high cost of the short-range three-body repulsive interactions.

5.3. Screening by Small Ions (Regime VI). Surface counterions start to dominate the screening of the surface charge for the higher surface charge densities $\sigma > \sigma_{ion}$.[21,23] In this range of surface charge densities there are three different regions in the adsorbed layer (see Figure 6b). Close to the charged surface the polymer density is of the order of $a^{-3} f^{1/2}$. The polymer density $\rho(z)$ is proportional to $a^{-3}\sqrt{f\varphi(z)}$ at intermediate length scales. It is constant ($\rho \approx a^{-3}\tau$) in the outer part of the adsorbed layer. The thickness of the adsorbed layer D at low salt concentrations (regime VIL) saturates at

$$D \approx au^{-1/2} f^{-3/4}, \quad \text{low salt } r_D > au^{-1/2} f^{-3/4} \qquad (80)$$

while at high salt concentrations it is of the order of the Debye radius r_D up to logarithmic corrections.[21,23]

However, the intermediate regime (regime V) with surface charge densities $\sigma_\theta < \sigma < \sigma_{ion}$ exists only if there is more than one charged monomer in the thermal blob ξ_T or for the effective temperatures $\tau < \sqrt{f}$. For higher effective temperatures $\tau > \sqrt{f}$ the system directly crosses over into the counterion-controlled regime when the Gouy−Chapman length due to surface charge $1/l_B\sigma$ becomes of the order of the layer thickness D given by eqs 63 and 65 for low and high salt regimes, respectively. The thickness of the adsorbed layer saturates at

$$D \approx \frac{a}{\sqrt{uf\tau}}, \quad \text{low salt } r_D > \frac{a^3\sigma}{f\tau}, \tau > \sqrt{f} \qquad (81)$$

in this "screening by small ions" regime at low salt concentrations.

6. Adsorption Diagram in the Case of Strong van der Waals Interactions

In sections 3−5 above we have neglected the effect of the van der Waals interaction between the charged

surface and the polymer backbone. The effective interaction between the adsorbing surface and a monomer in a solvent is[37]

$$W(z) \approx -kT\frac{a^3}{z^3}A_{\text{eff}} \tag{82}$$

where A_{eff} is the effective Hamaker constant for polymer surface interaction.

In regime IV of the adsorption diagram (Figure 3) the 3-D adsorbed layer is built of the blobs with constant size $\xi_T \approx a/\tau$. Let us estimate the van der Waals attraction of the blob closest to the charged surface

$$W(\xi_T) \approx \xi_T^2\int_a^{\xi_T}\rho(z)\,W(z)\,dz \approx -kT\frac{A_{\text{eff}}}{\tau}\left(1-\frac{a}{\xi_T}\right) \approx -kT\frac{A_{\text{eff}}}{\tau} \tag{83}$$

This attractive interaction is controlled by the low limit of the integral, proving that only monomers in contact with an adsorbing surface contribute to this type of interactions. Taking this into account, we can rewrite the last equation as the energy per contact $kT\epsilon_{VW}$ (the sticking energy of the monomer to the adsorbing surface) times the number of contacts n_{cont} per blob. Since the statistics of the chain on length scales smaller than the blob size ξ_T is Gaussian, the number of contacts n_{cont} of a blob with the number of monomers $g_T \approx \xi_T^2/a^2$ in it with adsorbing surface is $\sqrt{g_T} \approx \tau^{-1}$.

$$W(\xi_T) \approx -kT\frac{A_{\text{eff}}}{\tau} \approx -kTA_{\text{eff}}\sqrt{g_T} \approx -kT\epsilon_{VW}\sqrt{g_T} \tag{84}$$

Thus, the sticking energy per contact $kT\epsilon_{VW}$ is proportional to A_{eff}.

The van der Waals attraction can be neglected if it is weaker than electrostatic attraction of the first layer of thermal blobs

$$|W(\xi_T)| < kTfg_T|\varphi(0)| \tag{85}$$

However, in regime IV the structure of the adsorbed layer is controlled by the monomer−monomer interactions rather than electrostatic attraction to a charged surface, and it will not be affected by the van der Waals attraction as long as it is weaker than kT per thermal blob ($|W(\xi_T)| < kT$). This leads to the following inequality for the sticking energy

$$\epsilon_{VW} < g_T^{-1/2} \approx \tau \tag{86}$$

In regimes V and VI of the adsorption diagram (Figure 3) the energy of the closest to the surface blobs is always of the order of the thermal energy kT. In this case the sticking energy ϵ_{VW} should be

$$\epsilon_{VW} < g^{-1/2}(0) \tag{87}$$

in order to safely neglect the effects of the van der Waals attraction to the surface. The number of monomers in these blobs $g(0)$ is always smaller than that in the thermal blob g_T, because these blobs are compressed by electrostatic attraction to the charged surface. Thus, if the sticking energy ϵ_{VW} is smaller than τ, we can neglect the effect of the van der Waals interactions in the entire 3-D region of the adsorption diagram (Figure 3).

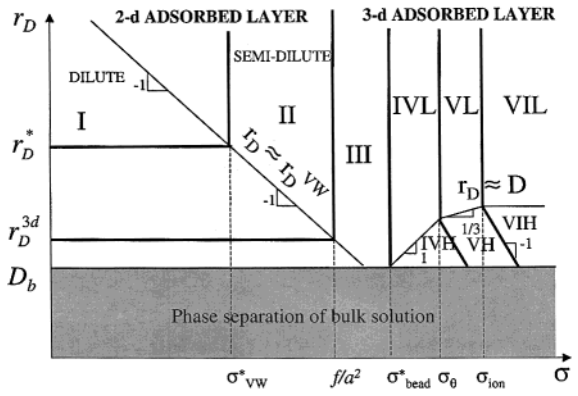

Figure 7. Adsorption diagram of polyelectrolyte chains in a salt solution as a function of surface charge density σ and Debye radius r_D in the case of strong van der Waals interactions.

In the case of the 2-D adsorbed layers ($\sigma < \sigma^*_{\text{bead}}$) the adsorbed polyelectrolyte chains have a necklace-like structure. The beads on the necklace will undergo wetting/dewetting transition as the strength of the van der Waals interactions of the polymer backbone with adsorbing surface increases. This transition occurs if the surface energy gain due to increase the number of contacts between polymer backbone and the adsorbing surface is higher than the surface energy loss due to increase in the area of the polymer−solvent interface. The energy difference per unit area of the spreading bead is

$$\delta\gamma \simeq -kT\frac{\epsilon_{VW}\sqrt{g_T}}{\xi_T^2} + \frac{kT}{\xi_T^2} \simeq \frac{kT}{a^2}(-\epsilon_{VW}\tau + \tau^2) \tag{88}$$

where the first term describes the energy difference per unit area between the polymer−surface interface $\gamma - kT\epsilon_{VW}\tau/a^2$ and the surface−solvent interface γ, and the last one is the surface energy per unit area of polymer−solvent interface. The beads spread if the energy difference $\delta\gamma$ is negative. This occurs for the values of the sticking energy ϵ_{VW} larger than the effective temperature τ.

Now let us discus how the adsorption diagram will change if the sticking energy ϵ_{VW} is larger than the effective temperature τ. Our results for this case are summarized in Figure 7.

6.1. Three-Dimensional Adsorbed Layer. We begin our discussion of the adsorption diagram from 3-D adsorbed layers. In this case the strong van der Waals attraction of the polymer backbone to the adsorbing surface controls the layer structure near the adsorbing surface. In the vicinity of the charged surface polyelectrolytes form de Gennes' carpet[38] with polymer density profile given by the following equation

$$\rho(z) \simeq \frac{1}{a^2(\xi_{vw} + z)} \tag{89}$$

where ξ_{vw} is the size of the closest to the surface blob (adsorption blob). The size of this blob can be found from the condition that its van der Waals interaction with adsorbing surface is of the order of the thermal energy

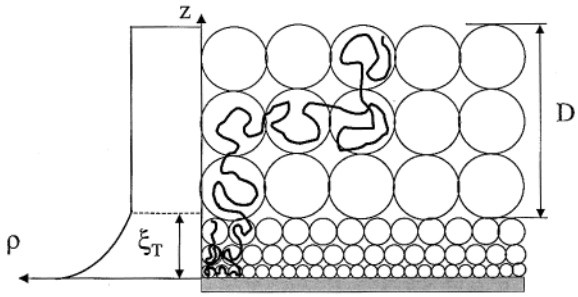

Figure 8. Polymer density profile and layer structure in the 3-D adsorbed layer in the case of strong van der Waals interactions (regime IV).

kT or $\epsilon_{VW}g(0)^{1/2} \approx 1$. This leads to the following expression for the blob size

$$\xi_{vw} \approx a/\epsilon_{VW} \tag{90}$$

In regime IV of the adsorption diagram (see Figure 7) this de Gennes' carpet ends at the distance z from a charged surface where the polymer density $\rho(z)$ becomes comparable with polymer density τ/a^3 inside thermal blob ξ_T (see Figure 8). This takes place at the distance z of the order of the size ξ_T of the thermal blob. The polymer excess within the layer of thickness ξ_T results in the screening of the surface charge by the amount $fa^{-2}\ln(\epsilon_{VW}/\tau)$ leading to the effective surface charge density

$$\sigma_{eff} \approx \sigma - \frac{f}{a^2}\ln\left(\frac{\epsilon_{VW}}{\tau}\right) \tag{91}$$

that the rest of the adsorbed polyelectrolytes "feel". However, in the 3-D adsorbed regimes the surface charge density σ is always higher than f/a^2. Thus, the presence of van der Waals interactions does not significantly affect the properties of the adsorbed layer.

A similar analysis of the effect of the van der Waals interactions can be carried out in regimes V and VI of the adsorption diagram (see Figure 7). In both of these regimes the van der Waals attractions will perturb the structure of the adsorbed layer at length scales z smaller than the size of the first blob $\xi(0)$ (see eq 78 for the blob size $\xi(0)$ in regime V and $\xi(0) \approx af^{-1/2}$ in regime VI). At these length scales the polymer density profile will be given by eq 89 while at the distances $z > \xi(0)$ the structure of the adsorbed layer will remain the same as without van der Waals interactions (see section 5).

However, in the case of strong van der Waals interactions ($\epsilon_{VW} > \tau$) adsorbed polyelectrolytes form 3-D adsorbed layer even at the surface charge densities σ below σ^*_{bead} (regime III in Figure 7). The structure of the adsorbed layer at these surface charge densities is similar to the one in regime IV discussed above. At the length scales $z < \xi_T$ the adsorbed chains form de Gennes's carpet with polymer density given by eq 89. At length scales larger than the thermal blob size ξ_T the polymer density is constant and is equal to τa^{-3}. The thickness of this layer of constant density can be obtained by substituting the effective surface charge density σ_{eff} (eq 91) into eq 63

$$D \approx r_D \operatorname{arcsinh}\left(\frac{a^3}{f\tau r_D}\left(\sigma - \frac{f}{a^2}\ln\left(\frac{\epsilon_{VW}}{\tau}\right)\right)\right) \tag{92}$$

The outer layer of thickness D disappears completely

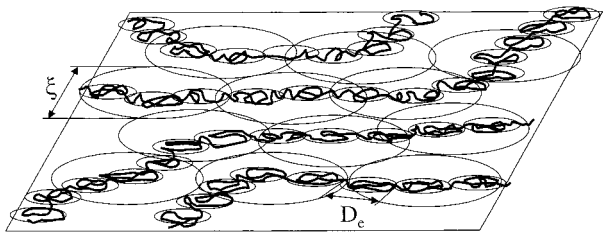

Figure 9. Schematic sketch of the adsorbed layer in *semidilute 2-D* regime in the case of strong van der Waals interactions.

at the surface charge density $\sigma \approx fa^{-2}\ln(\epsilon_{VW}/\tau)$. At this value of the surface charge density the thickness of the adsorbed layer is of the order of the thermal blob size ξ_T. As the surface charge density σ decreases further ($\sigma < fa^{-2}\ln(\epsilon_{VW}/\tau)$) the thickness of the adsorbed layer D reaches the size of the adsorption blob ξ_{vw} exponentially fast[39] and saturates there at lower surface charge densities. In fact, the system crosses over into 2-D semidilute adsorbed layer at surface charge density $\sigma \approx fa^{-2}$ at low salt concentrations. However, for higher salt concentrations $r_D < a\epsilon_{VW}^2/f^2u$, at which the electrostatic interactions per monomer in the adsorbed layer f^2ur_D/a are weaker than average monomer−surface interactions ϵ_{VW}^2, the adsorbed polyelectrolytes form a monolayer of overlapping chains with thickness ξ_{vw}, maximizing the number of polymer surface contacts, even for surface charge densities σ lower than fa^{-2}.

6.2. Semidilute Two-Dimensional Wigner Liquid (Regime II). For lower surface charge densities ($\sigma < fa^{-2}$) adsorbed polyelectrolytes arrange themselves into a two-dimensional semidilute polyelectrolyte solution with the distance between chains ξ and chain thickness of the order of the adsorption blob size ξ_{vw} controlled by the van der Waals attraction of the polymer backbone to the adsorbing surface (see Figure 9). The intrachain electrostatic repulsion leads to chain stretching along the adsorbing surface on length scales larger than electrostatic blob[3,4,6] size D_e (see Figure 9). The conformation of a chain inside the electrostatic blob is almost unperturbed by electrostatic interactions and by two-body monomer−monomer attraction with the number of monomers in it being $g_e \approx (D_e/a)^2$. The size of the electrostatic blob D_e containing g_e monomers can be found by comparing the electrostatic energy of a blob $e^2g_e^2f^2/\epsilon D_e$ with the thermal energy kT. This leads to the electrostatic blob size

$$D_e \approx a(uf^2)^{-1/3} \tag{93}$$

and the number of monomers in it

$$g_e \approx (uf^2)^{-2/3} \tag{94}$$

At the length scales smaller than ξ the polyelectrolyte configuration is that of a fully extended array of g_ξ/g_e electrostatic blobs of contour length ξ

$$\xi \approx \frac{g_\xi}{g_e}D_e \approx ag_\xi(uf^2)^{1/3} \tag{95}$$

To calculate the total free energy of the adsorbed layer, we will once again divide the electrostatic contribution to the total free energy into the repulsive and attractive ones and add to it the contribution from the short-range van der Waals interactions. With these

modifications the free energy of the adsorbed layer is

$$\frac{F}{kT} \approx Sl_B r_D f g_\xi \left(\frac{f g_\xi}{2\xi^4} \exp\left(-\frac{\xi}{r_D}\right) - \frac{\sigma}{\xi^2} \right) - S\epsilon_{VW}{}^2 \frac{g_\xi}{\xi^2} \quad (96)$$

Minimizing this free energy F with respect to the Wigner−Seitz cell size ξ and keeping in mind that $g_\xi \approx \xi/(u^{1/3} f^{2/3} a)$, we obtain the equation that defines the cell size as a function of the Debye radius r_D

$$\frac{f^{1/3}}{u^{1/3}\xi a}\left(1 + \frac{\xi}{2r_D}\right)\exp\left(-\frac{\xi}{r_D}\right) \approx \sigma + \frac{\epsilon_{VW}{}^2}{l_B r_D f} \quad (97)$$

It follows from the last equation that the cell size can be obtained by balancing the electrostatic repulsion between chains either with their attraction to the oppositely charged surface (the first term on the right-hand side of eq 97) or with their nonelectrostatic attraction to the adsorbing surface (the second term on the right-hand side of eq 97). The crossover between two stabilizing mechanisms takes place across the line

$$r_D^{VW} \approx \frac{\epsilon_{VW}{}^2}{l_B \sigma f} \quad (98)$$

At low salt concentrations ($r_D > r_D^{VW}$) the size of the cell

$$\xi \approx \frac{f^{1/3}}{u^{1/3} a \sigma}, \quad r_D > r_D^{VW} \quad (99)$$

is inversely proportional to the surface charge density σ. The surface overcharging $\delta\sigma$ in this regime

$$\delta\sigma \approx \frac{\epsilon_{VW}{}^2}{l_B r_D f}, \quad r_D > r_D^{VW} \quad (100)$$

is inversely proportional to the Debye radius r_D and is independent of the surface charge density σ.

At higher salt concentrations ($r_D < r_D^{VW}$) the solution of eq 97 is

$$\xi \approx r_D \frac{u^{2/3} f^{4/3}}{\epsilon_{VW}{}^2}, \quad r_D < r_D^{VW} \quad (101)$$

In this regime the distance between chains ξ scales linearly with the Debye screening length r_D. Thus, the distance between chains decreases as salt is added to the solution. The 2-D electrostatic blobs start to overlap at the salt concentrations for which the Wigner−Seitz cell size ξ is of the order of the electrostatic blob size D_e. This occurs for the following value of the Debye radius r_D

$$r_D^{3d} \approx a \frac{\epsilon_{VW}{}^2}{u f^2}, \quad r_D < r_D^{VW} \quad (102)$$

At this salt concentration ($r_D \approx r_D^{3d}$) the polymer surface coverage Γ

$$\Gamma(r_D^{3d}) \approx \frac{g_\xi}{\xi^2} \approx \frac{\epsilon_{VW}{}^2}{l_B r_D^{3d} f^2} \approx \frac{1}{a^2}, \quad r_D \le r_D^{3d} \quad (103)$$

reaches its maximum possible value and stays unchanged for higher salt concentrations (in regime III of Figure 7 for the interval of the surface charge densities $\sigma < fa^{-2}$).

The surface overcharging by adsorbed polyelectrolytes in the interval of salt concentrations ($r_D^{3d} < r_D < r_D^{VW}$) is

$$\delta\sigma \approx \frac{f g_\xi}{\xi^2} - \sigma \approx \frac{\epsilon_{VW}{}^2}{l_B r_D f} \quad (104)$$

and it increases with increasing the salt concentration.

As the surface charge density σ decreases in the regime of low salt concentrations ($r_D > r_D^{VW}$) or as the salt concentration decreases in the regime of high salt concentrations ($r_D < r_D^{VW}$), the size of the Wigner−Seitz cell ξ (see eqs 98 and 101) increases and reaches the size $L \approx aN(uf^2)^{1/3}$ of the polyelectrolyte chain at the surface charge density

$$\sigma^*_{VW} \approx \frac{1}{a^2 u^{2/3} f^{1/3} N}, \quad r_D > r_D^{VW} \quad (105)$$

and at the value of the Debye radius

$$r^*_D \approx aN \frac{\epsilon_{VW}{}^2}{u^{1/3} f^{2/3}}, \quad r_D < r_D^{VW} \quad (106)$$

These values of the surface charge density σ^*_{VW} and of the Debye radius r^*_D define the boundary between 2-D semidilute (II) and dilute (I) regimes.

6.3. Dilute Two-Dimensional Wigner Liquid (Regime I). The total free energy of the adsorbed layer in a dilute regime is the sum of the contributions from all chains due to electrostatic and short-range van der Waals interactions

$$\frac{F}{kT} \approx Sl_B r_D f N \left(\frac{1}{2}\frac{fN}{R^4} \exp\left(-\frac{R}{r_D}\right) - \frac{\sigma}{R^2} \right) - S\epsilon_{VW}{}^2 \frac{N}{R^2} \quad (107)$$

The dependence of the Wigner−Seitz cell size R on the salt concentration is derived by minimizing the total free energy with respect to R. The equilibrium cell size is the solution of the following equation

$$\frac{fN}{R^2}\exp\left(-\frac{R}{r_D}\right)\left(1 + \frac{1}{4}\frac{R}{r_D}\right) \approx \sigma + \frac{\epsilon_{VW}{}^2}{l_B r_D f} \quad (108)$$

At low salt concentrations $r_D > r_D^{VW}$ the size R of the Wigner−Seitz cell has very weak dependence on the Debye screening length r_D. Thus, on the scaling level, we can assume that at low salt concentrations

$$R \approx \sqrt{fN/\sigma}, \quad r_D > r_D^{VW} \quad (109)$$

At low salt concentrations we can expand the left-hand side of eq 108 in the power series of R/r_D. After this expansion eq 108 reduces to

$$\frac{fN}{R^2}\left(1 - \frac{3}{4}\frac{R}{r_D}\right) \approx \sigma + \frac{\epsilon_{VW}{}^2}{l_B r_D f} \quad (110)$$

Within this approximation the overcharging of the charged surface by adsorbed polyelectrolyte chains is

$$\delta\sigma \approx \frac{fN}{R^2} - \sigma \approx \frac{\epsilon_{VW}^2}{l_B r_D f}, \quad r_D > r_D^{VW} \tag{111}$$

When the Debye radius r_D becomes smaller than r_D^{VW} the electrostatic repulsion between adsorbed polyelectrolyte chains is balanced by their van der Waals attraction to adsorbing surface. The Wigner−Seitz cell size R that minimizes the total free energy eq 107 is

$$R \approx \sqrt{r_D l_B N}\,\frac{f}{\epsilon_{VW}}, \quad r_D < r_D^{VW} \tag{112}$$

Thus, the cell size R is proportional to the square root of the Debye radius r_D. The effective surface charge density in this high salt concentrations regime is

$$\delta\sigma \approx \frac{fN}{R^2} - \sigma \approx \frac{\epsilon_{VW}^2}{l_B r_D f}, \quad r_D < r_D^{VW} \tag{113}$$

It has the same functional form as in the semidilute regime (see eq 104) and can be much larger than the bare surface charge density σ.

7. Conclusion

We have presented a scaling analysis of the adsorption of hydrophobic polyelectrolytes at the oppositely charged surfaces from dilute polymer solutions. In the case of hydrophilic surfaces, when the sticking energy ϵ_{VW} per monomer due to van der Waals interactions with charged surface is smaller than the effective temperature τ ($\epsilon_{VW} < \tau$), the structure of the adsorbed layer in the *dilute* (regime I in Figure 3) and *semidilute string-controlled* (regime II in Figure 3) regimes is qualitatively similar to that for adsorption of polyelectrolytes from a Θ-solvent for polymer backbone.[22] In these regimes the adsorbed necklaces form a two-dimensional strongly correlated Wigner liquid. At low salt concentrations the size of the corresponding Wigner−Seitz cells is determined by the electroneutrality condition of these cells while at higher salt concentrations it is proportional to the Debye radius r_D (up to logarithmic corrections). The chains are localized inside the layer of thickness $D \approx (l_B f N \sigma)^{-1}$ (see Figure 10) for surface charge densities smaller than σ_{def} and the value of the Debye radius r_D larger than the transverse size of the necklace $\sqrt{\langle R_\perp^2 \rangle}$. For higher surface charge densities $\sigma > \sigma_{def}$ and smaller values of the Debye radius $r_D < \sqrt{\langle R_\perp^2 \rangle}$ the thickness of an adsorbed chain D is determined by the balance of the energy gain due to electrostatic attraction and the confinement entropy loss due to chain localization. The thickness of the adsorbed chain D decreases with increasing surface charge density as $\sigma^{-1/3}$ (see Figure 10) and is independent of the degree of polymerization N. The thickness of the adsorbed layer $D \approx D_b$ saturates at the surface charge density $\sigma \approx \sigma_{sat}$.

In the interval of the surface charge densities where the size of the Wigner−Seitz cell is smaller than the bare length of the string l_{str} between two neighboring beads but larger than the bead size D_b (regime III in Figure 3) there is on average one bead per each correlation cell. In this regime the adsorbed layer resembles 2-D Wigner liquid of charged colloidal particles for which the Wigner−Seitz cell size is inversely proportional to square root of the surface charge density $\sigma^{-1/2}$ at low salt concentrations.

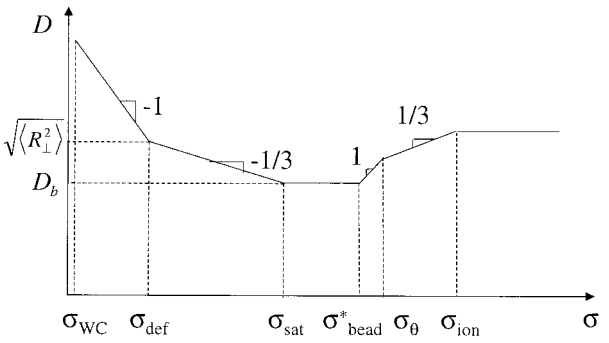

Figure 10. Dependence of the thickness of the adsorbed layer D on the surface charge density σ in salt-free solution (logarithmic scales).

The crossover to the 3-D adsorbed layer occurs at the surface charge density σ of the order of σ^*_{bead} at which beads begin to overlap. For higher surface charge densities in the interval $\sigma^*_{bead} < \sigma < \sigma_\theta$ (regime IV in Figure 3) the thickness of the adsorbed layer grows linearly with the surface charge density σ (see Figure 10). The monomer density in the adsorbed layer is constant and equal to τa^{-3}.

If the surface charge density increases further ($\sigma_\theta < \sigma < \sigma_{ion}$) (regime V in Figure 3), the equilibrium density profile in the adsorbed layer is determined by the balance between electrostatic attraction of charged monomers to the surface and short-range monomer−monomer repulsion in the layers close to the surface and by the balance of the two-body attraction and three-body repulsion further away from it. On length scales $z < h$ the polyelectrolytes form a self-similar carpet with polymer density decaying as $(D - z)^2$ (see Figure 6a). At the intermediate length scales ($h < z < D$) the monomer density in the adsorbed layer is constant and is equal to that inside a polymeric globule $a^{-3}\tau$.

For very high surface charge densities ($\sigma > \sigma_{ion}$) (regime VI in Figure 3) the surface counterions dominate the screening of the surface potential near the wall. There are three different regions in the adsorbed layer (see Figure 6b). Close to the charged surface counterions dominate the surface screening, and the monomer density is almost constant $\rho \approx a^{-3} f^{1/2}$ with one elementary charge per correlation blob. Further away from the charged surface the density profile in the two remaining layers is similar to the one described above.

The thickness of the 3-D adsorbed layer in the low salt concentration regime increases linearly with the surface charge density σ in the regime $\sigma^*_{bead} < \sigma < \sigma_\theta$ and grows as $\sigma^{1/3}$ for $\sigma_\theta < \sigma < \sigma_{ion}$. At very high surface charge densities ($\sigma > \sigma_{ion}$) layer thickness saturates at $a u^{-1/2} f^{-3/4}$. In the high salt concentration regimes the thickness of the adsorbed layer is proportional to the Debye screening length r_D.

For comparison, Figure 11 shows the dependence of the layer thickness of the adsorbed layer in the case of strong van der Waals interactions (hydrophobic surfaces ($\epsilon_{VW} > \tau$)). The thickness of the adsorbed chains stays constant equal to the size of the adsorption blob ξ_{VW} in the 2-D dilute (regime I in Figure 7) and semidilute (regime II in Figure 7) regimes. Then for the surface charge densities σ higher than $a^{-2} f$ it increases linearly with the surface charge density. Finally, at high surface charge densities $\sigma > \sigma^*_{bead}$ the surface charge density dependence of the layer thickness is the same as for

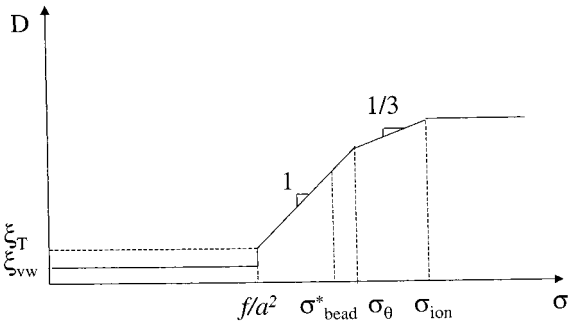

Figure 11. Dependence of the thickness of the adsorbed layer D on the surface charge density σ in salt-free solution in the case of strong van der Waals interactions (logarithmic scales).

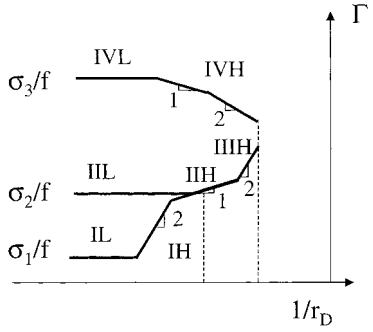

Figure 12. Dependence of polymer surface coverage Γ on salt concentration (reciprocal Debye radius) for polyelectrolyte adsorption at hydrophilic surface for three different surface charge densities $\sigma_1 < \sigma^*$, $\sigma_{sat} < \sigma_2 < f/a^2$, $\sigma^*_{bead} < \sigma_3 < \sigma_\theta$ (logarithmic scales).

polyelectrolyte adsorption at hydrophilic surface (see Figure 10).

It is useful to estimate the typical σ values for the boundaries between different regimes in the adsorption diagram (Figures 10 and 11). Consider polyelectrolyte chains consisting of $N \approx 10^2$ Kuhn segments with size $a \approx 4A$, $\tau \simeq 0.1$, and fraction $f \approx 0.1$ of these segments charged, adsorbing from an aqueous solution with the Bjerrum length $l_B = 7A$. In this case the boundaries between regimes in the adsorption diagram are $\sigma_{WC} \approx 10^{-5}\ A^{-2}$, $\sigma^* \approx 4 \times 10^{-4}\ A^{-2}$, $\sigma^*_{bead} \approx 2 \times 10^{-3}\ A^{-2}$, and $\sigma_{ion} \approx 10^{-2}\ A^{-2}$.

The polymer adsorbed amount

$$\Gamma \approx \frac{\sigma + \delta\sigma}{f} \tag{114}$$

can either increase or decrease with addition of salt depending on the surface charge density. For the surface charge densities σ below σ^*_{bead} in the regions where the adsorbed polyelectrolytes form 2-dimensional adsorbed layers, the polymer surface coverage grows with increasing salt concentration (see Figure 12). The addition of salt screens electrostatic repulsion between adsorbed polyelectrolytes, making the increase of the adsorbed amount energetically favorable. This increase of polymer surface coverage continues until the adsorption/desorption threshold where the coverage decreases to zero.

Qualitatively different dependence of the surface coverage on salt concentration is predicted for surface charge densities $\sigma > \sigma^*_{bead}$ (see Figure 12). In this range of surface charge densities the adsorbed polyelectrolytes form a 3-D adsorbed layer. There are two different effects that contribute to the decrease of the polymer surface excess with addition of salt. Inside the 3-D adsorbed layer the addition of salt decreases the polymer adsorbed amount, because salt ions are also participate in screening of the surface charge. Additional decrease in the polymer surface excess comes from the edge of the adsorbed layer.

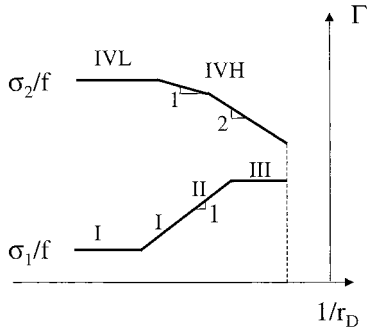

Figure 13. Dependence of polymer surface coverage Γ on salt concentration (reciprocal Debye radius) for polyelectrolyte adsorption at hydrophobic surface for two different surface charge densities $\sigma_1 < \sigma^*_{VW}$, $\sigma^*_{bead} < \sigma_2 < \sigma_\theta$ (logarithmic scales).

In the case of polyelectrolyte adsorption at hydrophobic surfaces the polymer surface coverage increases with increasing salt concentration in the dilute, semidilute, and 3-D regimes for surface charge densities $\sigma < fa^{-2}$ (see regimes I, II, and III (for $\sigma < fa^{-2}$) in Figure 7). In these regimes it is inversely proportional to the Debye radius r_D (see Figure 13). This growth in polymer adsorbed amount continues until $r_D \geq r_D^{3d}$. At higher salt concentrations ($r_D < r_D^{3d}$) the surface coverage saturates at a^{-2}. At high surface charge densities $\sigma > f/a^2$ the polymer surface coverage decreases with salt concentration in the same way as in the 3-D adsorbed layer without van der Waals interactions discussed in the previous paragraph.

The linear dependence of the polymer adsorbed amount on the square root of salt concentration ($\Gamma \sim r_D \sim \sqrt{\rho_{salt}}$) was reported by Papanhuyzen et al.[41] for adsorption of poly(styrenesulfonate) on crystals of poly(oxymethylene) and by Marra et al.[42] for adsorption of poly(styrenesulfonate) on weakly charged silica at pH ≈ 2. A similar salt dependence of the polymer adsorbed amount was also reported by Yim et al.,[43] who studied the adsorption of poly(styrenesulfonate) to the air/water interface. The adsorption of poly(styrenesulfonate) at the air/water interface is due to a strong surface attraction arising from the low surface energy of polystyrene in comparison with that of water. At low salt concentrations the adsorbed chains form a single dense layer with almost flat chain configurations. This dependence of the polymer adsorbed amount on salt concentration is in a good qualitative agreement with our prediction for polyelectrolyte adsorption on hydrophobic surfaces (see regimes I, II, and III of the adsorption diagram Figure 7 where adsorption of polyelectrolyte chains is due to strong affinity of polymer backbone to the adsorbing surface).

Thus, our theory of adsorption of hydrophobic polyelectrolytes at charged surfaces gives a qualitatively reasonable interpretation of the experimental results. Of course, our theory does not cover all aspects of polyelectrolyte adsorption. We leave aside the question of the effect of the difference in the dielectric constants of solvent and adsorbing substrate on polyelectrolyte adsorption. However, the difference in the dielectric constants of the adsorbing substrate and the solvent can

only lead to some quantitative corrections and will not change the qualitative picture of polyelectrolyte adsorption described in the present paper. The detailed analysis of this effect requires special consideration and will be addressed in a separate publication.

Acknowledgment. Authors are grateful to the National Science Foundation for the financial support under Grants ECS-0103307 and DMR-0102267, and to the donors of the Petroleum Research Fund, administrated by the American Chemical Society, for financial support under Grant 37018-AC7.

Appendix

Consider the fluctuations $h(x,y)$ of the thickness D of the adsorbed layer in the direction normal to polymer−solvent interface. For slowly varying fluctuations of the charged polymer−solvent interface the additional free energy of the undulating interface with respect to that of the flat one is

$$\frac{\delta F(\{h(x,y)\})}{kT} \approx \frac{1}{2\xi_T^2}\int dx\, dy\, (h_x^2(x,y) + h_y^2(x,y)) + \frac{l_B\rho^2 f^2}{2}\int dx\, dy \int dx_1\, dy_1 \times \frac{h(x,y)\, h(x_1,y_1) \exp\left(-\frac{\sqrt{(x-x_1)^2+(y-y_1)^2}}{r_D}\right)}{\sqrt{(x-x_1)^2+(y-y_1)^2}} \quad (115)$$

where the first term describes the surface free energy of undulating interface due to increase of its surface area and the second one is the energy of electrostatic interaction between the charges $dq(x_i,y_i) = \rho f h(x_i,y_i)\, dx_i\, dy_i$ at the polymer−solvent interface. The charge $dq(x_i,y_i)$ is positive for $h(x_i,y_i) > 0$ and negative for $h(x_i,y_i) < 0$, leading to the effective attraction between hills ($h(x_i,y_i) > 0$) and valleys ($h(x_i, y_i) < 0$) that flatters the interface. Introducing the Fourier transformation $h(q)$

$$h(\vec{q}) = \int dx\, dy\, h(x,y) \exp(-i(q_x x + q_y y)) \quad (116)$$

where $\vec{q}$ is a two-dimensional vector with coordinates q_x and q_y, one can rewrite the expression for the free energy of undulating interface with electrostatic interactions as follows

$$\frac{\delta F(\{h(\vec{q})\})}{kT} \approx \frac{1}{2\xi_T^2}\int dq_x\, dq^y \left(q^2 + \frac{2\pi l_B \rho^2 f^2 \xi_T^2}{\sqrt{q^2 + r_D^{-2}}}\right) h(\vec{q})\, h(-\vec{q}) \quad (117)$$

where we introduced $q^2 = q_x^2 + q_y^2$. The probability of fluctuations $h(\vec{q})$ is proportional to $\exp(-\delta F(\{h(\vec{q})\})/kT)$. In the Gaussian approximation the mean-square value of the interface fluctuations $h(\vec{q})$ is

$$\langle h(\vec{q})\, h(-\vec{q})\rangle \approx \xi_T^2 \left(q^2 + \frac{1}{\sqrt{q^2 + r_D^{-2}} D_b^3}\right)^{-1} \quad (118)$$

where we used the following relation $2\pi l_B \rho^2 f^2 \xi_T^2 \approx a^{-3} u f^2 \approx D_b^{-3}$. The correlation function $\langle h(\vec{q})\, h(-\vec{q})\rangle$ has the maximum at the length scales $2\pi/q$ of the order of the bead size D_b. The mean-square roughness of the interface about its flat configuration is given by

$$\langle h(x,y)^2\rangle = \frac{\xi_T^2}{(2\pi)^2}\int dq_x\, dq_y \left(q^2 + \frac{1}{\sqrt{q^2 + r_D^{-2}} D_b^3}\right)^{-1} \approx \xi_T^2 \ln\left(\frac{D_b}{\xi_T}\right) \quad (119)$$

where we choose an upper limit of the integral to be ξ_T^{-1} due to the finite thickness of the polymer−solvent interface proportional to ξ_T. Thus, the typical fluctuations of the thickness of the adsorbed layer D are of the order of the thermal blob size ξ_T.

The analysis presented above shows that the solution eq 61 of the linearized Poisson−Boltzmann eq 59 for adsorbed layer with uniform density is stable significantly below the bead overlap surface charge density σ^*_{bead} up to the surface charge density $\sigma \approx f/a^2$ where the thickness of the adsorbed layer D becomes comparable with the interface roughness ξ_T.

We also have to check that this solution has higher energy than the Wigner liquid of beads. The free energy per unit area of the adsorbed layer with uniform density is

$$\frac{F_{3d}}{S} \approx kT\left(\frac{\tau^2}{a^2} - \frac{l_B a^3 \sigma^3}{f\tau}\right) \quad (120)$$

where the first term is the surface energy of polymer−solvent interface and the second one is the energy of electrostatic interactions within the adsorbed layer. The surface energy of the polymer−solvent interface (the first term on the right-hand side of eq 120) dominates over the energy of electrostatic interactions (the second one on the right-hand side of eq 120) for the surface charge densities σ below σ^*_{bead}.

The free energy per unit area of the Wigner liquid of beads also has two major contributions one is due to self-energy of the beads that includes beads surface and electrostatic energies (at equilibrium these two terms are of the same order of magnitude) and the electrostatic attraction of a bead to the oppositely charged background

$$\frac{F_{beads}}{S} \approx kT\left(\frac{\tau^2}{a^2}\frac{D_b^2}{\xi_b^2} - \frac{l_B m_b f \sigma}{\xi_b}\right) \quad (121)$$

In the interval of the surface charge densities $\sigma < \sigma^*_{bead}$ the first term on the right had side of eq 121 is bigger than the second one. Thus, the adsorbed layer with structure of Wigner liquid of beads has lower free energy per unit area than the adsorbed layer with uniform polymer density as long as the cell size ξ_b is bigger than the bead size D_b. This is true for the surface charge densities $\sigma < \sigma^*_{bead}$. At the surface charge density $\sigma \approx \sigma^*_{bead}$ there is a first-order phase transition between the Wigner liquid of beads and uniform adsorbed layer.

References and Notes

(1) *Polyelectrolytes*; Hara, M., Ed.; Marcel Dekker: New York, 1993.
(2) Schmitz, K. S. *Macroions in Solution and Colloidal Suspension*; VCH: Weinheim, 1993.
(3) de Gennes, P.-G.; Pincus, P.; Velasco, R. M.; Brochard, F. *J. Phys. (Paris)* **1976**, *37*, 1461.

(4) de Gennes, P.-G. *Scaling Concepts in Polymer Physics*; Cornell University Press: Ithaca, NY, 1979.
(5) Khokhlov, A. R.; Khachaturian, K. A. *Polymer* **1982**, *23*, 1742.
(6) Dobrynin, A. V.; Colby, R. H.; Rubinstein, M. *Macromolecules* **1995**, *28*, 1859.
(7) Dobrynin, A. V.; Rubinstein, M.; Obukhov, S. P. *Macromolecules* **1996**, *29*, 2974.
(8) Solis, F. J.; Olvera de la Cruz, M. *Macromolecules* **1998**, *31*, 5502.
(9) Dobrynin, A. V.; Rubinstein, M. *Macromolecules* **1999**, *32*, 915.
(10) Micka, U.; Holm, C.; Kremer, K. *Langmuir* **1999**, *15*, 4033.
(11) Lyulin, A. V.; Dunweg, B.; Borisov, O. V.; Darinskii, A. A. *Macromolecules* **1999**, *32*, 3264.
(12) Chodanowski, P.; Stoll, S. *J. Chem. Phys.* **1999**, *111*, 6069.
(13) Micka, U.; Kremer, K. *Europhys. Lett.* **2000**, *49*, 189.
(14) Castelnovo, M.; Sens, P.; Joanny, J.-F *Eur. Phys. J. E* **2000**, *1*, 115.
(15) Balazs, A. C.; Singh, C.; Zhulina, E.; Pickett, G.; Chern, S. S.; Lyatskaya, Y. *Prog. Surf. Sci.* **1997**, *55*, 181.
(16) Vilgis, T. A.; Johner, A.; Joanny, J.-F. *Eur. Phys. J. E* **2000**, *2*, 289.
(17) Tamashiro, M. N.; Schiessel, H. *Macromolecules* **2000**, *33*, 5263.
(18) Netz, R. R.; Joanny, J.-F. *Macromolecules* **1999**, *32*, 9026.
(19) Nguyen, T. T.; Grosberg, A. Yu.; Shklovskii, B. I. *Phys. Rev. Lett.* **2000**, *85*, 1588. *J. Chem. Phys.* **2000**, *113*, 1110.
(20) Joanny, J.-F.; Castelnovo, M.; Netz, R. *J. Phys.: Condens. Matter* **2000**, *12*, A1.
(21) Dobrynin, A. V.; Deshkovskii, A.; Rubinstein, M. *Phys. Rev. Lett.* **2000**, *84*, 3101.
(22) Dobrynin, A. V.; Deshkovskii, A.; Rubinstein, M. *Macromolecules* **2001**, *34*, 3421.
(23) Dobrynin, A. V. *J. Chem. Phys.* **2001**, *114*, 8145.
(24) Rouzina, I.; Bloomfield, V. *J. Phys. Chem.* **1996**, *100*, 9977.
(25) Perel, V. I.; Shklovskii, B. I. *Physica A* **1999**, *274*, 446.
(26) Shklovskii, B. I. *Phys. Rev. Lett.* **1999**, *82*, 3268.
(27) Varoqui, R. *J. Phys. II* **1993**, *3*, 1097.
(28) Borukhov, I.; Andelman, D.; Orland, H. *Europhys. Lett.* **1995**, *32*, 499.
(29) Joanny, J.-F. *Eur. Phys. J. B* **1999**, *9*, 117.
(30) Lord Rayleigh *Philos. Mag.* **1882**, *14*, 182.
(31) This definition of the adsorption/desorption transition corresponds to the ground-state dominance approximation. In this approximation a polymer chain considered to be adsorbed if there is discrete level in the chain energetic spectrum well separated from its continuous spectrum. See for review: Grosberg, A. Yu.; Khokhlov, A. R. *Statistical Physics of Macromolecules*; AIP Press: Melville, NY, 1994
(32) For the Odijk−Skolnick−Fixman model of the electrostatic persistence length in salt solutions[33,34] the electrostatic persistence length l_p is due to intrachain electrostatic repulsion and is proportional to the square of the Debye radius r_D. Considering a necklace as the polymer chain with the effective bond length equal to the length of a string l_{str} connecting two neighboring beads carrying the charge $m_b f$, we can rewrite the Odijk−Skolnick−Fixman expression for polyelectrolyte persistence length[33,34] $l_p \approx [l_B(m_b f)^2 r_D^2]/l_{str}^2 \approx r_D^2/\xi_T$, for $r_D > l_{str}$. The crossover to a rigid chain behavior occurs when the electrostatic persistent length l_p is of the order of the chain size L_{nec}. This takes place at the value of the Debye radius r_D proportional to the transversal chain size $\sqrt{\langle R_\perp^2 \rangle}$. For larger values of the Debye radius the chain can be viewed as a charged rod of length L_{nec}. Polyelectrolyte chains desorb when the electrostatic attraction between the charged surface and a section of size l_p is of the order of thermal energy kT: $|W_{ads}| \approx kTl_B\sigma f g_\xi l_p \approx kT$. The desorption transition takes place at the Debye screening length $r_D^{des} \approx (a/u^{1/2}\tau^{3/2}\sigma)^{1/3}$, for $r_D > l_{str}$.
(33) Odijk, T. *J. Polym. Sci., Polym. Phys. Ed.* **1977**, *15*, 477.
(34) Skolnick, J.; Fixman, M. *Macromolecules* **1977**, *10*, 944.
(35) The electrostatic part of the globular free energy has two terms. One is associated with the electrostatic interaction between charged monomers within the globule, and the second one is due to formation of the electrical double layer near the globular surface. The bulk contribution may be estimated as the electrostatic self-energy of a bead of size r_D and carrying a charge $f\rho r_D^3$ multiplied by the number of such beads in the globule volume $N/(\rho r_D^3)$: $W_{el}^{glob} \approx kTN(\tau u f^2 r_D^2)/a^2$. This contribution to the free energy is smaller than one due to short-range monomer−monomer interaction $kTN\tau^2$ by the factor $(r_D^2\xi_T/D_b^3)$ and can be neglected. The energy of the electrical double layer can be estimated as the electrostatic energy of the capacitor of thickness r_D with the surface charge density $f\rho r_D$ and the surface area R_{glob}^2: $W_{el}^{surf} \approx kTl_B r_D (f\rho r_D)^2 R_{glob}^2 \approx kTR_{glob}^2(uf^2\tau^2 r_D^3)/a^5 \approx kTR_{glob}^2(\tau^2/a^2)(r_D/D_b)^3$. This surface contribution to the globular free energy is weaker than the surface energy term due to polymer/solvent interface $kTR_{glob}^2\tau^2/a^2$ for the values of the Debye radius smaller than the bead size D_b and can be omitted from the globular free energy as well.
(36) Grosberg, A. Yu.; Khokhlov, A. R. *Statistical Physics of Macromolecules*; AIP Press: New York, 1994.
(37) Israelachvilli, J. N. *Intermolecular and Surface Forses*; Cornell University Press: Ithaca, NY, 1985.
(38) de Gennes, P. G. *Macromolecules* **1981**, *14*, 1637.
(39) The exponential dependence of the layer thickness on the surface charge density $D \approx \xi_{vw} \exp(\sigma a^2/f)$ is due to the neutralization condition of the surface charge by adsorbed polyelectrolytes $\sigma \approx f\int_0^D dz/[a^2(\xi_{vw} + z)] = fa^{-2} \ln(D/\xi_{vw})$.
(40) The two-body monomer−monomer attraction between two adsorption blobs with $g_{vw} \approx \epsilon_{VW}^{-2}$ monomers $-\tau a^3 g_{vw}^2/\xi_{vw}^3 \approx -\tau\sqrt{g_{vw}} \approx -\tau/\epsilon_{VW}$ is always weaker than that of three-body contacts $a^6 g_{vw}^3/\xi_{vw}^6 \approx 1$ for adsorption at hydrophobic surfaces $\epsilon_{VW} > \tau$.
(41) Papenhuyzen, J.; Fleer, G. J.; Bijsterbosh, B. H. *J. Colloid Interface Sci.* **1985**, *104*, 530.
(42) Marra , J.; van der Schee, H. A.; Fleer, G. J.; Lyklema, J. In *Adsorption in Solutions*; Ottiwel, R., Rochester, C. H., Smith, A. L., Eds.; Academic Press: New York, 1983; p 245.
(43) Yim, H.; Kent, M.; Matheson, A.; Ivkov, R.; Satija, S.; Majewski, J.; Smith, G. S. *Macromolecules* **2000**, *33*, 6126.

MA0114943